International Journal of Microwave and Wireless Technologies

cambridge.org/mrf

A novel defect ground structure for decoupling closely spaced *E*-plane microstrip antenna array

Zicheng Niu, Hou Zhang, Qiang Chen and Tao Zhong

Air Force Engineering University, Xi'an, China

Industrial and Engineering Paper

Cite this article: Niu Z, Zhang H, Chen Q, Zhong T (2019). A novel defect ground structure for decoupling closely spaced *E*-plane microstrip antenna array. *International Journal of Microwave and Wireless Technologies* **11**, 1069–1074. https://doi.org/10.1017/S1759078719000801

Received: 27 November 2018
Revised: 5 May 2019
Accepted: 8 May 2019
First published online: 31 May 2019

Key words:
Closely spaced antenna; defect ground structure; *E*-plane microstrip antenna; isolation enhancement; mutual coupling

Author for correspondence:
Zicheng Niu, E-mail: nzc585@126.com

Abstract

In this paper, a novel decoupling technique for closely spaced *E*-plane patch antennas using defect ground structure (DGS) is proposed. The electric field coupling between the antennas is suppressed by etching DGS which consists of a pair of rectangular slots and four stubs on the ground plane. Moreover, unlike the other methods, the DGS is not etched in the middle of the antennas but loaded along the outer edge of the radiated patch. Thus, through the adopted technology the distance between the antenna elements is reduced and the isolation is increased. To validate the improvements by adopting the proposed technology, the array with DGS loading has been fabricated and then measured. The measurement results show that designed antennas have 95 MHz 10-dB impedance bandwidth, which is 25 MHz higher than that of the antenna without DGS. More importantly, isolation improvements have been increased from 8.5 to 31.3 dB by using the decoupling technique when the antennas are placed with a 0.032 λ_0 edge-to-edge distance, where λ_0 is the free-space wavelength. Therefore, this technique can be widely applied to improve isolation in a compact and low profile antenna system.

Introduction

Microstrip antenna has the advantages of low profile, lightweight, and easy processing, so they are widely used in wireless communication systems. In multiple-input multiple-output (MIMO) system, two closely placed antenna elements get mutually coupled due to electromagnetic interactions. The high mutual coupling leads to the deterioration of antenna performance, including mismatching impedance and degrading radiation efficiency. So it is especially important to reduce the mutual coupling between antenna elements in the MIMO wireless communication system.

In recently published literature, several approaches were proposed to reduce the mutual coupling between two antenna elements. In [1–3], by placing a decoupling surface above the antenna array, the reflected wave is used to cancel the coupling between the antenna elements, thereby achieving the purpose of improving the isolation. However, the decoupling surface typically has a distance of 0.5 λ_0 from the antenna array, increasing the profile of the antenna. In [4], Z. Y. Wang places the meta-surface on the antenna array and reduces the coupling using the band-stop characteristic of the square split ring resonators. Although the profile is reduced compared with the decoupling surface, the matching of antennas needs to be readjusted because the medium parameters are changed. In [5], the polarization conversion isolator is loaded in the 1×2 microstrip antenna array and the isolation is improved 19.6 dB through controlling the polarization of the coupling field. Nevertheless, after the isolator is loaded between the two antennas, the distance between the antenna elements is increased.

In MIMO systems, the spacing of antenna elements is a critical part of the design. Multiple antennas are difficult to integrate into a limited space, so the distance between the antennas needs to be as small as possible. Defect ground structure (DGS) is usually etched on the ground plate of the antenna to change the distribution of effective dielectric constant of the substrate, to change the distributed inductance and capacitance of microstrip line based on dielectric so that such transmission lines have band-gap and slow wave characteristics in [6, 7]. Previous papers [8–20] have documented the use of DGS to improve the performance of the antenna. In [13], the isolation of the antenna is improved by etching two 2C-shaped defective structures between the antennas, so that the port isolation exceeds 20 dB in the operating band. The S-shaped periodic defected ground structure is etched between the antenna elements to reduce mutual coupling in [14]. Through observation, we can find that the distance between the two antennas in the [13] and [14] is 0.31 λ_0 and 0.24 λ_0, respectively. It is concluded that the conventional practice which etching the defective structure on the ground plate between the antennas undoubtedly increases the distance between the antennas. In [20], the DGS is placed along the edge of the radiation patch to improve radiation properties. Through summarizing

© Cambridge University Press and the European Microwave Association 2019

CAMBRIDGE UNIVERSITY PRESS

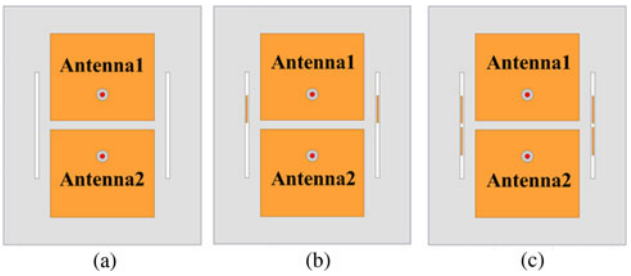


Fig. 1. Evolution of the proposed DGS design. (a) Stage 1: The DGS only consists of a pair of rectangular grooves. (b) Stage 2: the DGS with a pair of rectangular grooves and two stubs. (c)Stage 3: The DGS consists of a pair of rectangular grooves and four stubs.

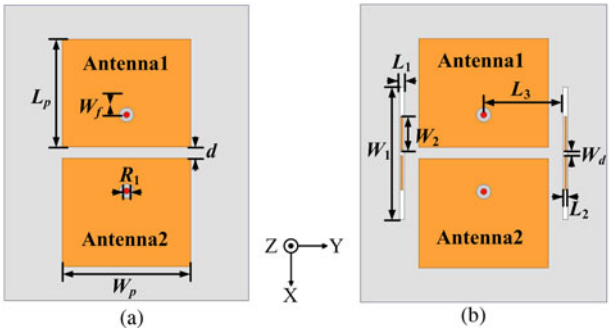


Fig. 3. (a) Schematic diagram of the two-element microstrip antenna array without DGS; (b) Schematic diagram of the antenna array with DGS.

the electric field distribution in the substrate, the decoupling mechanism can be easily demonstrated.

In this paper, a pair of rectangular grooves with four stubs is etched along the outer edge of the 1×2 *E*-plane microstrip antennas. In this way, the problem of excessive spacing caused by conventional etching of the DGS between the antennas is avoided. After simulation and measurement, the isolation between the antennas is improved by 22.8 dB when the antennas are placed with a 0.032 λ_0 edge-to-edge distance, achieving a good decoupling purpose.

Antenna design

Three different DGS structures are shown in Fig. 1 to expound the design process of DGS. In order to avoid the problem of spaces increasing caused by slot etched in the ground plane between the antennas, we placed the DGS along the outer edge of the *E*-plane microstrip antenna array.

The principle and process of the design can be explained by analyzing the electric field in the substrate. As can be seen from Fig.2(a), the electric field in the dielectric substrate is coupled from the antenna1 to the antenna2. After etching a pair of rectangular slots on the floor, part of the electric field in the substrate is bound to the slots in Fig. 2(b). This phenomenon indicates that the proposed way of loading DGS can effectively change the distributed capacitance of the ground plane, thus preventing electric field coupling. In order to avoid resonant effect and strengthen the ability of DGS to restrain energy coupling, stubs are added into the rectangular slots. Adding a stub in the rectangular slot respectively, most of the electric field is suppressed around the stubs. It can be seen from Fig. 2(c) that the electric field is reduced at the outer edge of the antenna2 compared to Figs 2(a) and (b). To maintain the matching of antennas and guarantee the symmetry of the decoupling structure, two stubs are added in the rectangular groove in Fig.2(d). The electric field coupled to antenna2 by antenna1 is almost entirely bound around the reformative DGS, and the outer edge of antenna2 has almost no electric fields coupled to it.

The antenna array without DGS and with DGS geometry is shown in Figs 3(a) and (b), respectively. As shown in Fig. 3(b), the DGS is etched along the outer edge of the patch. The antenna array is printed on a 1 mm thick substrate with dielectric constant 2.65 and loss tangent 0.001. And the antennas are excited by a coaxial connector with 50 Ω impedance. After loading DGS, the position of the feed point remains unchanged. Both of them working in the same band (center frequency 4 GHz) are placed with edge-to-edge distance $d = 2.4\ mm$ (0.032 λ_0). The dimension of the antenna array with DGS is: $W_p = 22.2\ mm$, $L_p = 26.5\ mm$, $W_f = 4.5\ mm$, $R_1 = 1.2\ mm$, $d = 2.4\ mm$, $W_1 = 26.9\ mm$, $L_1 = 1\ mm$, $W_2 = 6.9\ mm$, $L_2 = 0.4\ mm$, $L_3 = 16.25\ mm$, and $W_d = 1.3\ mm$. The overall size of the array is $60.8 \times 50.5 \times 1\ mm^3$.

The antenna array with and without DGS is numerically simulated by HFSS 15.0. Figures 4(a) and (b) show the current distributions on the ground plane with and without DGS, respectively. When port 1 is excited, the DGS inhibits the propagation of most coupling currents. Figure 5 shows the simulated reflection and transmission coefficient of the microstrip antenna array with and without DGS. As can be seen in Fig. 5, the 10-dB impedance bandwidth of the antenna array with DGS (3.93–4.03 GHz) is larger than that of antenna array without DGS (3.99–4.04 GHz), and the antenna matching is better, although the center frequency is slightly offset. It can be concluded from Fig. 5 that the isolation between antenna elements at the center frequency is only

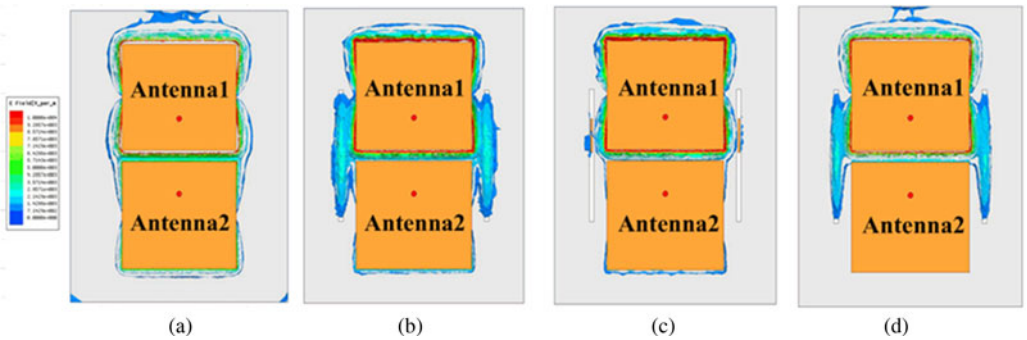


Fig. 2. Simulated substrate electric-filed contours (a) without DGS; (b) stage1; (c) stage2, and (d) stage3.

https://doi.org/10.1017/S1759078719000801 Published online by Cambridge University Press

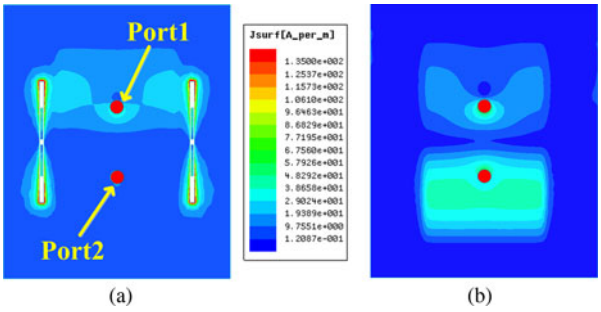


Fig. 4. Current distributions on the ground plane (a) with DGS and (b) without DGS.

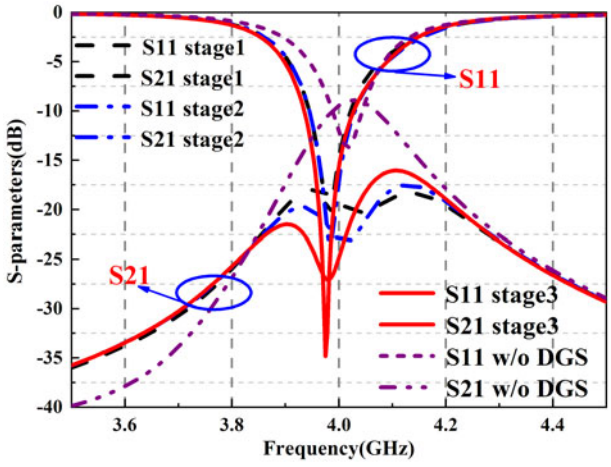


Fig. 5. Simulated S-parameters for stage 1–3 and array without DGS.

8.9 dB, this is because the spacing between the antennas is very small (only 0.032 λ_0). After the DGS is craved on the ground plane, the isolation of the antenna array at the center frequency increases to 27 dB (improved by 18.1 dB).

The reflection and transmission characteristics of the microstrip antenna array with the DGS during various stages of evolution are shown in Fig. 5. It can be seen that with the increase of the number of stubs loaded in the rectangular grooves, the central frequency is not only offset, but also matching becomes better and better. More importantly, the isolation between antennas is also getting higher and higher. Compared with the array without DGS, the center frequency of the antenna is slightly offset, but it can be seen that the isolation and antenna matching have been greatly improved.

Parameters analysis

Figures 6(a) and (b) show the trend of S_{11} and S_{21} with the length of rectangular slot-W_1. With the increase of the W_1, the distribution inductance increases, which leads to the maximum isolation to lower frequency. However, when it is reduced to a certain length, the maximum isolation within the working bandwidth disappears, and the decoupling effect of the DGS is lost. By optimization, the matching of antennas and the isolation between elements can be achieved with satisfactory results. The length of the stub-W_2 has little effect on the reflection coefficient, as can be seen in Fig. 6(c). However, since adding a pair of stubs will increase the distribution inductance, we can see in Fig. 6(d) that the change of W_2 will cause the change of the maximal isolation. The distance between the rectangular slot and the center of the antenna is particularly important to suppress the propagation of the coupled electric field at the radiation edge. Since the DGS

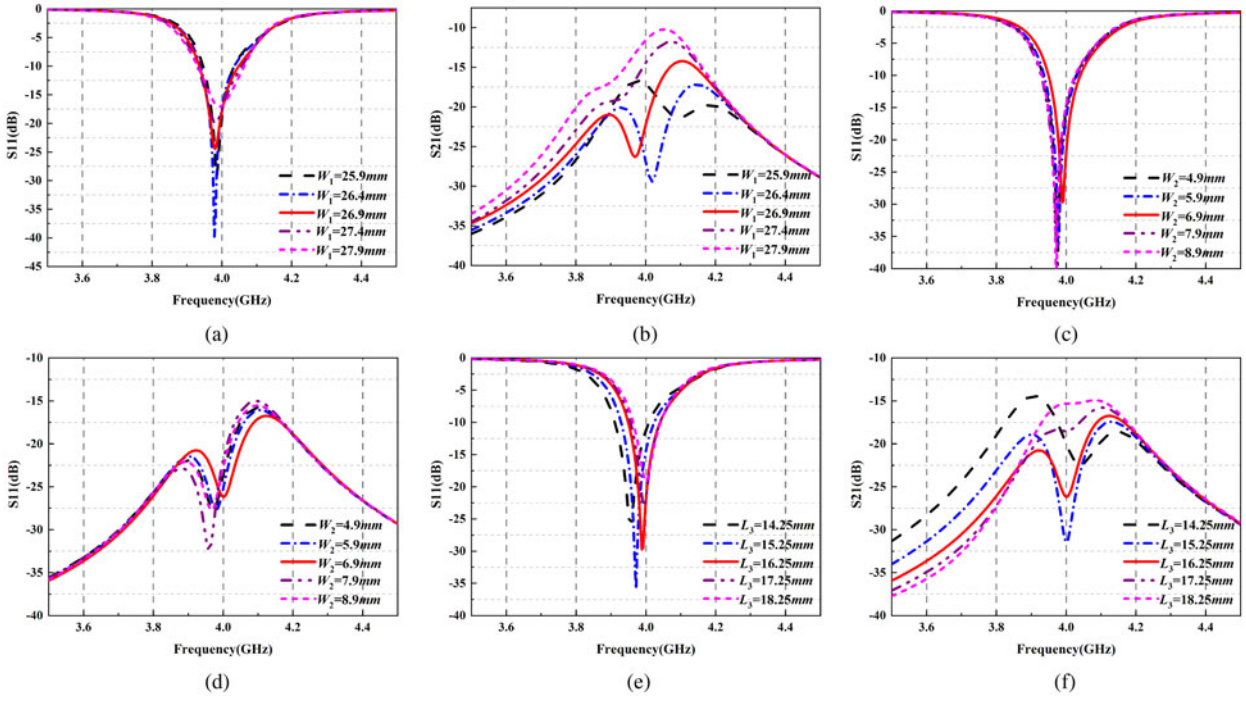


Fig. 6. Simulated S-parameters of the antenna array with DGS respect to different parameters: (a) S_{11} of the length of rectangular – W_1; (b) S_{21} of the length of rectangular – W_1; (c) S_{11} of the length of stub – W_2; (d) S_{21} of the length of stub – W_2; (e) S_{11} of the distance between the rectangular slot and the center of antenna – L_3; (f) S_{21} of the distance between the rectangular slot and the center of antenna – L_3.

https://doi.org/10.1017/S1759078719000801 Published online by Cambridge University Press

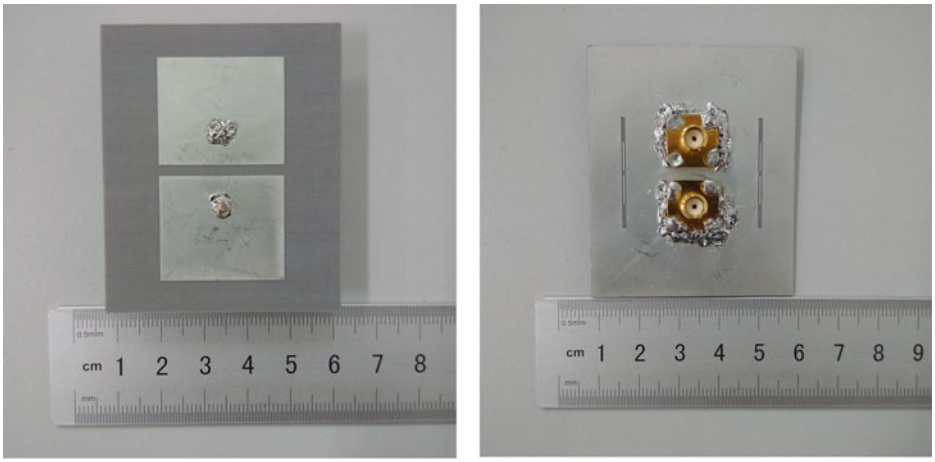


Fig. 7. Fabricated microstrip antenna array with DGS; (a) top view (b) bottom view.

changes the electric field distribution in the substrate, the electrical length of the radiation patch is changed, and the center frequency of the antenna tends to be high frequency as the L_3 increases in Fig. 6(e). When L_3 is small, the electric field bound by DGS interacts with the electric field generated by the radiation patch, which affects the antenna matching and the ability of the DGS to restrain the propagation of coupling electric fields. Figure 6(f) shows the change of the transmission coefficient of the antenna with L_3, and through optimization, it is learned that the transmission coefficient obtains the minimum value at the $L_3 = 15.25\ mm$, but at this time the resonant frequency of the antenna deviates from 4 GHz. Therefore, through comprehensive analysis, it is learned that when $L_3 = 16.25\ mm$, the antenna has excellent isolation at the central frequency.

Simulation and measurement results

The proposed antenna array with DGS is designed, constructed, and measured based on optimized parameter values. When the reflection coefficient was measured, the antenna 1 is excited, while the other is terminated with a 50 Ω load. Figure 7 shows the object of the designed microstrip antennas with DGS. Both the antenna1 and antenna2 are designed to work at 4 GHz frequency, and they are placed with edge-to-edge distance 0.032 λ_0, where λ_0 is the free-space wavelength at 4 GHz. The reflection

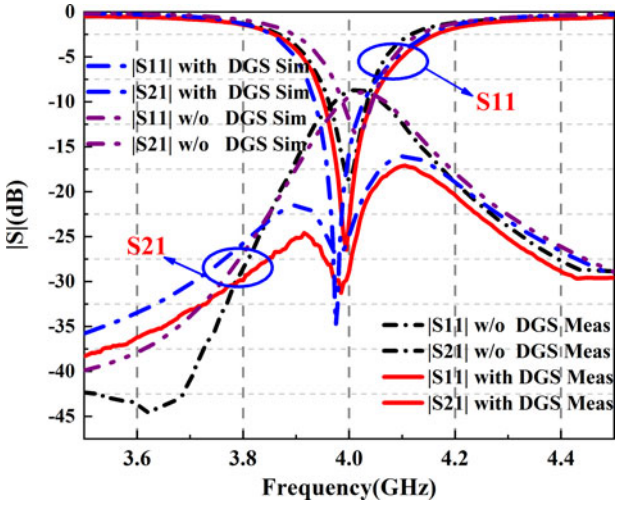


Fig. 8. Simulated S-parameter characteristics of the with and without DGS antenna array.

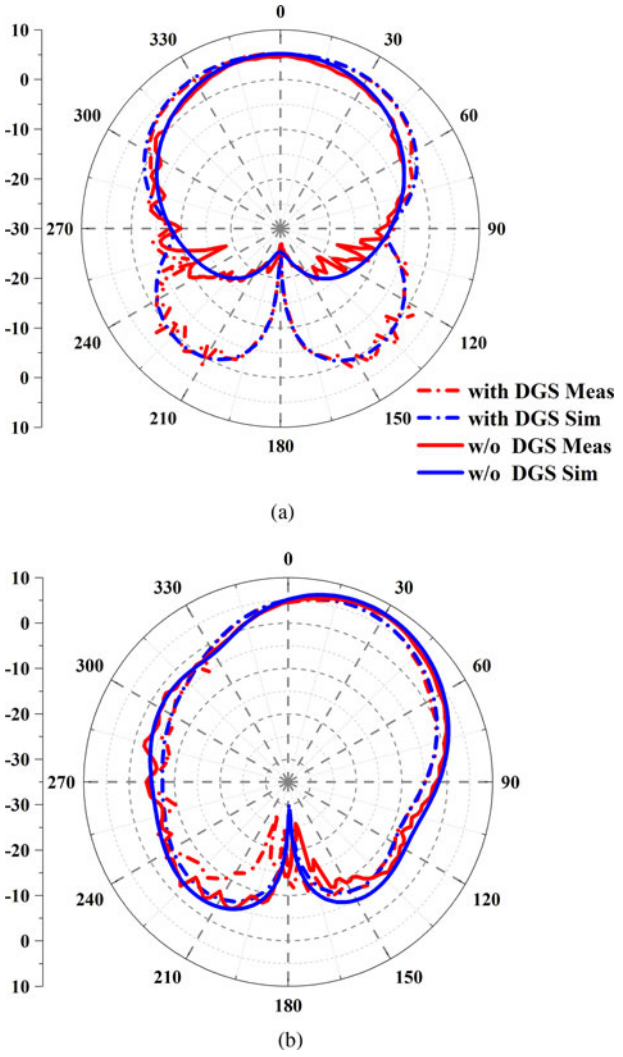


Fig. 9. Simulated and measured radiation pattern for the arrays at 4 GHz with and without DGS (antenna 1 excited and antenna 2 terminated by 50 Ω); (a) *xoz*-plane and (b) *yoz*-plane.

https://doi.org/10.1017/S1759078719000801 Published online by Cambridge University Press

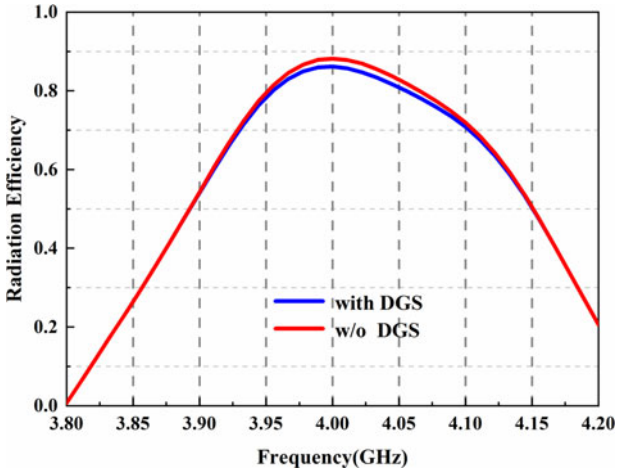


Fig. 10. Simulated radiation efficiency of the array with and without DGS.

Table 1. Performance comparison of the proposed DGS and other decoupling techniques used in recent published literature

Papers	Decoupling technique	f_o (GHz)	Edge to edge spacing (λ_0)	Maximum isolation improvement (dB)
[14]	DGS	2.57	0.24	40
[21]	Resonator	5.25	0.50	44
[22]	UC-EBG	5.05	0.22	16
[23]	PCR	3.5	0.07	26.2
Proposed	***DGS***	***4***	***0.032***	***22.8***

Bold italics significance is to emphasize the difference between the decoupling method proposed in this paper and other literatures.

coefficient and the transmission coefficient of the manufactured antenna are measured for a frequency range from 3.5 to 4.5 GHz. Figure 8 shows the simulated and measured S parameters of the microstrip antennas with and without DGS. On the whole, the changing trend of S parameters is the same as that of simulation results. According to Fig. 8, the measurement results show that the 10-dB impedance bandwidth of the antenna at 4 GHz is 95 MHz (3.950–4.045 GHz), which increases the bandwidth of the antenna by 20 MHZ compared to the non-loaded DGS. Nevertheless, due to the processing errors, the measured reflection coefficient is slightly different from the simulation results. In addition, after etching the DGS, the isolation between the antennas reached more than 20.1 dB within the −10 dB working bandwidth, with a maximum value of 31.3 dB: an increase of 22.8 dB is observed (from 8.5 to 31.3 dB).

The measured and simulated radiation patterns of the arrays are shown in Figs 9(a) and (b). According to Fig. 9, we can see that the measurement results are in good agreement with the simulation results. In addition, by comparing with the array without DGS, the main lobe direction of the antenna is not offset. Unfortunately, for the decoupling method of etching slots in the ground plate, the back lobe of the antenna will inevitably increase. As can be seen from Fig. 10, within the 10-dB impedance bandwidth, radiation efficiency of the antenna with DGS is only 0.1 lower than that without loading the DGS.

Table1 compares the proposed DGS in this paper with other decoupling techniques presented in the literature. Compared with the same mechanism of loading DGS, the proposed loading LDGS along the outer edge of the radiation patch effectively reduces the edge-to-edge distance. In contrast to other decoupling techniques, the proposed decoupling technique can achieve high isolation between antennas in the case of close antenna spacing. Through comparison, it can be concluded that this decoupling technique can be applied to the closely spaced microstrip antenna array.

Conclusion

In this paper, a novel DGS is proposed to enhance isolation between microstrip antenna elements. The DGS effectively inhibits the propagation of the electric fields to reduce mutual coupling. Moreover, the structure is etched along the outer edge of the radiation patch to reduce the spacing of the array. Through the simulations and measurements, the proposed DGS provides a maximum isolation enhancement of 22.8 dB with respect to the isolation passes from 8.5 to 33.1 dB within working bandwidth and the impedance bandwidth is increased by 20 MHz when the antennas are placed with a 0.032 λ_0 edge-to-edge distance.

References

1. **Wu KL, Chang N, Mei WX and Zhang ZY** (2017) Array-antenna decoupling surface. *IEEE Transactions on Antennas Propagation* **65**, 6728–6738.
2. **Wei CN and Wu KL** (2017) Array-antenna decoupling surfaces for Quasi-Yagi antenna arrays. *Antenna and Propagation & USNC/URSI National Radio Science Meeting*, pp. 2103–2104.
3. **Niu ZC, Zhang H, Chen Q and Zhong T** (2018) Isolation enhancement using a novel array-antenna decoupling surface for microstrip antennas. *Progress In Electromagnetics Research M* **72**, 49–59.
4. **Wang ZY, Zhao LY, Cai YM, Zheng SF and Yin YZ** (2018) A meta-surface antenna array decoupling (MAAD) method for mutual coupling reduction in a MIMO antenna system. *Scientific Reports* **8**, 1–9, no. 3152.
5. **Cheng YF, Ding X, Shao W and Wang BZ** (2017) Reduction of mutual coupling between patch antennas using a polarization-conversion isolator. *IEEE Antennas and Wireless Propagation Letters* **16**, 1257–1260.
6. **Jung S, Lim YK and Lee HY** (2008) A coupled-defected ground structure lowpass filter using inductive coupling for improved attenuation. *Microwave and Optical Technology Letters* **50**, 1541–1543.
7. **Zhu YZ, Zhang XJ, Li C, Li F and Fang GY** (2008) Novel compact meander-slot DGS with high quality factor. *Microwave and Optical Technology Letters* **50**, 3164–3169.
8. **Habashi A, Naurinia J and Ghbadi C** (2012) A rectangular defected ground structure for reduction of mutual coupling between closely spaced microstrip antennas. *in Proceedings of the 20th Iranian Conference on Electrical Engineering*, pp. 1347–1350.
9. **Biswas S and Guha D** (2013) Stop-band characterization of an isolated DGS for reducing mutual coupling between adjacent antenna elements and experimental verification for dielectric resonator antenna array. *International Journal of Electronics and Communications* **67**, 319–322.
10. **Hou DB, Xiao S, Wang BZ, Jiang L, Wang J and Hong W** (2009) Elimination of scan blindness with compact defected ground structures in microstrip phased array. *IET Microwaves. Antennas Propagation* **3**, 269–275.
11. **Veisee S, Asadi S and Hedayati MK** (2016) A novel compact defected ground structure and its application in mutual coupling reduction of a microstrip antenna. *Turkish Journal of Electrical Engineering & Computer Sciences* **24**, 3664–3670.
12. **Xiao S, Tang MC, Bai YY, Gao S and Wang BZ** (2011) Mutual coupling suppression in microstrip array using defected ground structure. *IET Microwaves, Antennas & Propagation* **5**, 1488–1494.

https://doi.org/10.1017/S1759078719000801 Published online by Cambridge University Press

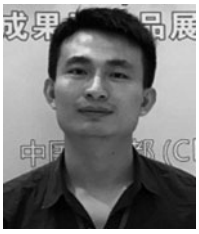
13. **Das G, Sharma A, Gangwar RK and Sharawi MS** (2018) Triple-port, two-mode based two element cylindrical dielectric resonator antenna for MIMO applications. *Microwave and Optical Technology Letter* **60**, 1566–1573.
14. **Wei K, Li JY, Wang L, Xing ZJ and Xu R** (2016) S-shaped periodic defected ground structures to reduce microstrip antenna array mutual coupling. *Electronics Letters* **52**, 1288–1290.
15. **Chen Q and Zhang H** (2018) Dual-patch polarization conversion metasurface-based wideband circular polarization slot antenna. *IEEE Access* **6**, 74772–74777.
16. **Khandelwal MK, Kanaujia BK, Dwari S, Kumar S and Gautam AK** (2016) Triple band circularly polarized microstrip antenna with defected ground structure for wireless applications. *International Journal of Microwave & Wireless Technologies* **8**, 943–953.
17. **Khandelwal MK, Kumar S and Kanaujia BK** (2018) Design, modeling and analysis of dual feed defected ground microstrip patch antenna with wide axial ratio bandwidth. *Journal of Computational Electronics* **17**, 1019–1028.
18. **Kanaujia BK, Khandelwal MK, Dwari S, Kumar S and Gautam AK** (2016) Analysis and design of compact high gain microstrip patch antenna with defected ground structure for wireless applications. *in Wireless Personal Communications* **91**, 661–678.
19. **Khandelwal MK, Kanaujia BK, Dwari S and Kumar S** (2014) Bandwidth enhancement and cross-polarization suppression in ultra-wideband microstrip antenna with defected ground plane. *Microwave and Optical Technology Letters* **56**, 2141–2146.
20. **Kumar C, Pasha MI and Guha D** (2017) Defected ground structure integrated microstrip array antenna for improved radiation properties. *IEEE Antennas and Wireless Propagation Letters* **16**, 310–312.
21. **Ghosh C-K** (2016) A compact 4-channel microstrip MIMO antenna with reduced mutual coupling. *International Journal of Electronics and Communications* **70**, 873–879.
22. **Yang X, Liu Y, Xu YX and Gong SX** (2017) Isolation enhancement in patch antenna array with Fractal UC-EBG structure and cross slot. *IEEE Antennas Wireless Propagation Letters* **16**, 2175–2178.
23. **Vishvaksenan KS, Mithra K, Kalaiarasan R and Raj KS** (2017) Mutual coupling reduction in microstrip patch antenna arrays using parallel coupled-line resonators. *IEEE Antennas Wireless Propagation Letters* **16**, 2146–2149.



Zicheng Niu was born in Hebei, China in 1996. He received the bachelor degree from Nanjing University of Posts and Telecommunications (NJUPT), Nanjing, China, in 2017. He is currently pursuing the master degree in electrical science and technology, Air Force Engineering University (AFEU), Xi'an, China. His research interests include MIMO antenna and array decoupling. E-mail address: nzc585@126.com.



Hou Zhang received his B.S., M.S., and Ph.D. degrees all in Electromagnetic Field and Microwave Technology from Xi'an Electronic and Engineering University, Air force Missile College, Xidian University, respectively. Dr. Zhang has been the session Chairs of PIERS and APEMC. He is currently interested in planar antennas and EMC. Prof. Zhang has published over 150 technical papers and authored/edited six books. He holds six granted/filed patents. E-mail address: warmer88@163.com



Qiang Chen was born in Jiangxi, China. He received the bachelor and master degree from Air Force Engineering University (AFEU), Xi'an, China, in 2011 and 2013, respectively. He is currently pursuing the Ph.D. degree in electrical science and technology, Air Force Engineering University (AFEU), Xi'an, China. His research interests include microwave circuits, antennas, and arrays. E-mail address: 1062620145@qq.com.



Tao Zhong was born in Hubei Province, China. He received the M.S. degree in electromagnetic field and microwave technology from Air Force Engineering University (AFEU), Xi'an, China, in 2016. Since 2017, he has been working towards the Ph.D. degree in electrical science and technology, AFEU, Xi'an, China. His research interests include leaky-wave antennas, transmission line, and array antenna. Email address: ztbull001@163.com.

https://doi.org/10.1017/S1759078719000801 Published online by Cambridge University Press